The EMBO Journal (2013) 32, 1141–1154
www.embojournal.org

TRANSPARENT PROCESS

THE EMBO JOURNAL

Human microcephaly protein CEP135 binds to hSAS-6 and CPAP, and is required for centriole assembly

Yu-Chih Lin[1,3], Ching-Wen Chang[1,3], Wen-Bin Hsu[1], Chieh-Ju C Tang[1], Yi-Nan Lin[1], En-Ju Chou[1,2], Chien-Ting Wu[1] and Tang K Tang[1,*]

[1]Institute of Biomedical Sciences, Academia Sinica, Taipei, Taiwan, ROC and [2]National Defense Medical Center, Graduate Institute of Life Sciences, Taipei, Taiwan, ROC

Centrioles are cylindrical structures that are usually composed of nine triplets of microtubules (MTs) organized around a cartwheel-shaped structure. Recent studies have proposed a structural model of the SAS-6-based cartwheel, yet we do not know the molecular detail of how the cartwheel participates in centriolar MT assembly. In this study, we demonstrate that the human microcephaly protein, CEP135, directly interacts with hSAS-6 via its carboxyl-terminus and with MTs via its amino-terminus. Unexpectedly, CEP135 also interacts with another microcephaly protein CPAP via its amino terminal domain. Depletion of CEP135 not only perturbed the centriolar localization of CPAP, but also blocked CPAP-induced centriole elongation. Furthermore, CEP135 depletion led to abnormal centriole structures with altered numbers of MT triplets and shorter centrioles. Overexpression of a CEP135 mutant lacking the proper interaction with hSAS-6 had a dominant-negative effect on centriole assembly. We propose that CEP135 may serve as a linker protein that directly connects the central hub protein, hSAS-6, to the outer MTs, and suggest that this interaction stabilizes the proper cartwheel structure for further CPAP-mediated centriole elongation.

The EMBO Journal (2013) **32,** 1141–1154. doi:10.1038/emboj.2013.56; Published online 19 March 2013
Subject Categories: cell & tissue architecture; cell cycle
Keywords: cartwheel; CENPJ; centrosome; centriole duplication; microcephaly

Introduction

The centrosome, which is the primary microtubule (MT)-organizing centre, is composed of two centrioles surrounded by an electron-dense matrix known as pericentriolar material. Centriole duplication involves the growth of a procentriole next to the proximal end of the parental centriole (Azimzadeh and Marshall, 2010; Nigg and Stearns, 2011; Brito *et al*, 2012; Gonczy, 2012). Recent studies have identified several key centrosome-associated proteins (ZYG-1/PLK4, SAS-5/Ana2/STIL, SAS-6, and SAS-4/CPAP) that are essential for centriole duplication in worms (O'Connell *et al*, 2001; Kirkham *et al*, 2003; Leidel and Gonczy, 2003; Leidel *et al*, 2005; Delattre *et al*, 2006; Pelletier *et al*, 2006), flies (Bettencourt-Dias *et al*, 2005; Peel *et al*, 2007; Rodrigues-Martins *et al*, 2007), and mammals (Kleylein-Sohn *et al*, 2007). In human cells, following activation of PLK4, several proteins essential for centriole duplication, including hSAS-6, CEP135, CPAP, γ-tubulin, and CP110, are recruited to the base of the daughter centriole (Kleylein-Sohn *et al*, 2007). PLK4, hSAS-6 and STIL have been reported to play important roles in regulating centriole duplication during early S phase. Excessive expression of each of the above proteins results in centriole amplification (Habedanck *et al*, 2005; Leidel *et al*, 2005; Tang *et al*, 2011; Arquint *et al*, 2012; Vulprecht *et al*, 2012). During S and G2 phases, centrioles start to elongate and increase their length (Kuriyama and Borisy, 1981). It has been reported that overexpression of CPAP or depletion of CP110 induces centriole elongation, suggesting that CPAP and CP110 play antagonistic roles in controlling centriole length (Kohlmaier *et al*, 2009; Schmidt *et al*, 2009; Tang *et al*, 2009). Further studies revealed that CPAP is required for the initiation of procentriole assembly and its subsequent elongation (Kohlmaier *et al*, 2009; Schmidt *et al*, 2009; Tang *et al*, 2009), while hPOC5 (Azimzadeh *et al*, 2009) and Ofd1 (Singla *et al*, 2010) appear to be essential for building the distal ends of centrioles.

Centrioles are usually composed of nine triplet MTs organized around a cartwheel-shaped structure; this structure is located at the proximal end next to the pre-existing centriole, and is required for new growth of the daughter centriole. In *Chlamydomonas*, two major components have been described in the cartwheel. Bld12, an orthologue of *C. elegans* SAS-6, has been shown to form the central hub and inner spokes (Nakazawa *et al*, 2007), while Bld10, an orthologue of human CEP135, was proposed to form the pinhead in the cartwheel (Hiraki *et al*, 2007). The studies from Bld10 truncation experiments and immunoelectron microscopy in *Chlamydomonas* revealed that the middle region of Bld10 is essential for centriole formation and large deletions of either the N-terminus or the C-terminus that interfere with this region cause detachment of the cartwheel spoke from the triplet MTs, suggesting that Bld10 may connect the cartwheel to the triplets (Hiraki *et al*, 2007). Interestingly, the *Bld10*-null mutant shows disorganized mitotic spindles and lacks centrioles (Matsuura *et al*, 2004), and Bld10 depletion in *Paramecium* causes defects in basal body formation (Jerka-Dziadosz *et al*, 2010). In contrast, the function of Bld10/CEP135 in *Drosophila* is not yet clear. Depletion of Bld10 in *Drosophila* S2 cells showed a partial inhibition of centriole duplication (Dobbelaere *et al*, 2008).

*Corresponding author. Institute of Biomedical Sciences, Academia Sinica, 128 Academia Road, Section 2, Taipei 11529, Taiwan, ROC. Tel.: +886 2 26523901; Fax: +886 2 27825573; E-mail: tktang@ibms.sinica.edu.tw
[3]These authors contributed equally to this work.

Received: 9 October 2012; accepted: 18 February 2013; published online: 19 March 2013

Ultrastructural analysis revealed that mutant flies lacking Bld10 assemble centrioles and form functional centrosomes. However, these flies produce immotile sperm whose axonemes are deficient in the central pair of MTs (Mottier-Pavie and Megraw, 2009). Further studies revealed that *Drosophila* Bld10/CEP135 is dispensable for cartwheel formation (Roque *et al*, 2013) and may control the formation of the flagellum central MT pair (Carvalho-Santos *et al*, 2012).

CEP135 was originally reported to be a coiled-coil centrosomal protein in mammalian cells (Ohta *et al*, 2002). It is concentrated within the proximal lumen of centrioles and is needed for the formation of supernumerary centrioles following PLK4 overexpression (Kleylein-Sohn *et al*, 2007). However, the molecular mechanism underlying the participation of CEP135 in centriole duplication in human cells has not been well characterized. Primary microcephaly (MCPH) is a genetically heterogeneous disorder for which at least nine causative genes have been identified. The known MCPH proteins, microcephalin (MCPH1), WDR62 (MCPH2), CDK5RAP2 (MCPH3), CEP152 (MCPH4), ASPM (MCPH5), CPAP/CENPJ (MCPH6), STIL/SIL (MCPH7), CEP135 (MCPH8), and CEP63, are all ubiquitously expressed and are localized to centrosomes for at least part of the cell cycle, suggesting that the centrosome is likely to play a central role in this disease (Thornton and Woods, 2009; Bettencourt-Dias *et al*, 2011). A recent study identified a homozygous single base-pair deletion in exon 8 of *CEP135*, resulting in a frameshift that changed glutamine to serine at amino-acid position 324, followed by a premature stop codon (Hussain *et al*, 2012); this suggests that the C-terminal domain of CEP135 is essential for its centrosomal function. This truncating mutation of *CEP135* causes primary microcephaly in humans, which is characterized by reduced brain size and intellectual disability. Further analysis of a patient's fibroblasts revealed an abnormal centrosome number, but the molecular basis of this effect is not yet clear (Hussain *et al*, 2012). In this study, we suggest a molecular basis for the functions of CEP135 in human cells and a possible explanation for how a mutation in the hSAS-6-interacting domain of CEP135 may interfere with centriole assembly in human cells.

Results

CEP135 is required for centriole duplication and proper mitotic spindle assembly

Bld10/CEP135 is essential for cartwheel formation and centriole duplication in *Chlamydomonas* and *Paramecium* (Hiraki *et al*, 2007; Jerka-Dziadosz *et al*, 2010) and is needed for the formation of supernumerary centrioles following PLK4 overexpression in human cultured cells (Kleylein-Sohn *et al*, 2007). However, Bld10/CEP135 does not appear to be required for centriole duplication in *Drosophila* (Roque *et al*, 2013). To examine whether CEP135 is essential for normal centriole duplication in human cells, endogenous CEP135 was depleted by specific siRNA duplexes (siCEP135-1 or siCEP135-2). As shown in Figure 1, both siRNAs significantly inhibited CEP135 expression, as demonstrated by western blotting (Figure 1A) and immunofluorescent staining (Figure 1B). Furthermore, most CEP135-depleted cells displayed either one centriole (~55% for siCEP135-1 and ~58% for siCEP135-2) or two centrioles (~34% for siCEP135-1 and ~31% for siCEP135-2), implying that CEP135 is required for normal centriole duplication in human cells (Figure 1C). We used siCEP135-1 (hereafter referred to as siCEP135) for all subsequent experiments. Intriguingly, CEP135 depletion also induced mitotic abnormalities, with significant increases in monopolar spindles (MoP, ~36%) and abnormal bipolar spindles (ABP, ~41%) (Figure 1D and 1E). Immunofluorescence analysis of CEP135-depleted cells revealed that most of the abnormal spindles had unusual centriole numbers (Figure 1F); these included three centrioles (2+1 pattern: two in one pole, one in the other; see Figure 1F-i, where the centriole is positivity stained by centrin), two centrioles (1+1 and 2+0 patterns; Figure 1F-ii and -iii), and one centriole (1+0 and monopolar; Figure 1F-iv and -v), implying that CEP135 is essential for proper mitotic spindle assembly, possibly via the regulation of faithful centriole duplication. Taken together, our results suggest that CEP135 is required for both centriole duplication and proper mitotic progression in mammalian cells.

CEP135 directly interacts with the cartwheel protein, hSAS-6

CEP135/Bld10 and SAS-6/Bld12 were reported to be the major components within the cartwheels of *Chlamydomonas* and *Paramecium* (Hiraki *et al*, 2007; Nakazawa *et al*, 2007; Jerka-Dziadosz *et al*, 2010), and SAS-6 was later shown to self-assemble into a ring-shape structure akin to the central hub of the cartwheel (Kitagawa *et al*, 2011; van Breugel *et al*, 2011). However, it was unclear whether CEP135 directly interacts with hSAS-6. To resolve this question, we performed immunoprecipitation (IP) experiments. We found that endogenous hSAS-6 was detected in complexes precipitated by an anti-CEP135 antibody, but not by a normal control IgG (Figure 2B), indicating that CEP135 and hSAS-6 may form an interacting complex *in vivo*. In support of this notion, interactions between ectopically expressed full-length myc-tagged CEP135 and EGFP-tagged hSAS-6 were also detected in co-IPs using antibodies against EGFP or myc (Figure 2C).

To further map the interaction domains of each protein, HEK 293T cells were transfected with a series of myc-tagged hSAS-6 truncation constructs, and cell lysates were analysed by IP followed by immunoblotting (IB) with the indicated antibodies. Using this approach, we first mapped the minimum region of hSAS-6 (residues 307–586) that interacts with CEP135 (Figure 2D). Unexpectedly, our fine interaction mapping using a yeast two-hybrid assay further narrowed down the CEP135-interacting region to residues 307–536 in hSAS-6 (Supplementary Figure S1A). Further co-IP experiments demonstrated that the anti-CEP135 antibody could co-precipitate hSAS-6-myc (307–536) with CEP135 (Supplementary Figure S1B). We did not initially observe a distinguishable co-IP band in Figure 2D (307–536), because hSAS-6-myc (307–536) is similar in size to a non-specific band (marked by a '#' in the figure) detected by the anti-myc antibody. We thus conclude that residues 307–536 comprise the minimum region through which hSAS-6 interacts with CEP135.

We next determined the hSAS-6-interacting region in CEP135. HEK 293T cells were co-transfected with constructs encoding a full-length EGFP-hSAS-6 plus a series of myc-tagged CEP135 truncation constructs, and IP experiments were performed using an anti-myc antibody. Our results

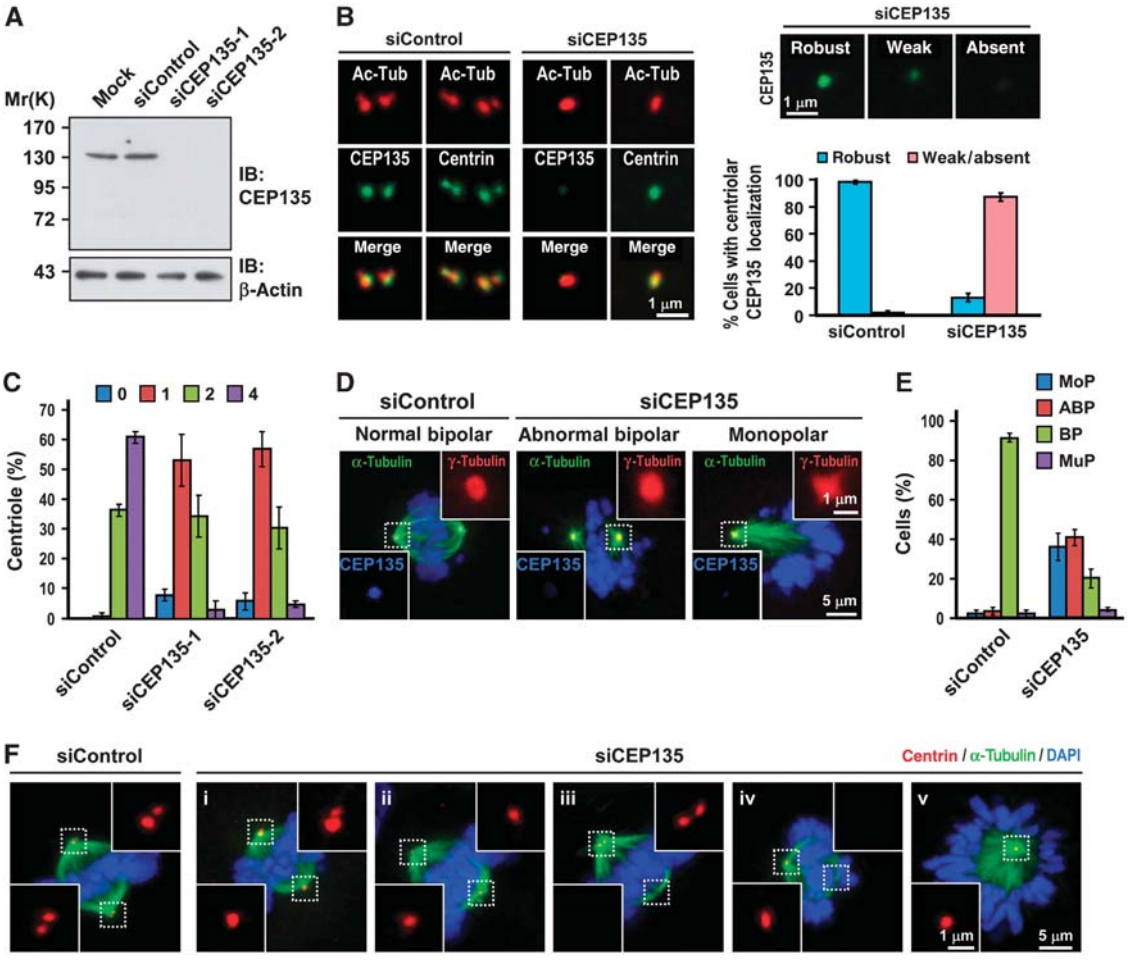

Figure 1 CEP135 is required for normal centriole duplication and maintains the integrity of mitotic spindles. U2OS cells were transfected with siControl or siCEP135 for 4 days, and analysed by immunoblotting (**A**) and immunofluorescence staining (**B**, **D**, and **F**) with the indicated antibodies. Depletion of CEP135 inhibits centriole duplication (**B**, **C**) and induces mitotic abnormalities (**D**, **E**) with irregular centriole numbers in mitotic cells (**F**). Histogram illustrating the percentages of siCEP135-treated cells showing the various centriole numbers (**C**, counted by centrin staining) and abnormal mitotic spindles (**E**) in cells. MoP, monopolar; ABP, abnormal bipolar; BP, normal bipolar; MuP, multipolar. Error bars represent mean ± s.d. of 100 cells from three independent experiments.

allowed us to map the hSAS-6-interacting domain to the C-terminal region of CEP135 (residues 416–1140; Figure 2E). To examine whether CEP135 directly interacts with hSAS-6, we performed *in vitro* GST pull-down assays. Full-length CEP135 proteins were synthesized *in vitro*, labelled with ^{35}S-methionine, and then incubated with either GST or GST-hSAS-6 full-length recombinant proteins. We found that only GST-hSAS-6 could specifically pull-down ^{35}S-methionine-labelled full-length CEP135 (Figure 2F). Together, our results suggest a direct interaction between hSAS-6 (residues 307–536) and CEP135 (residues 416–1140). A schematic of the interaction between CEP135 and hSAS-6 is shown in Figure 2A.

CEP135 directly binds to MTs

After cartwheel formation, MT triplets attach to the cartwheel for further centriole assembly. In human cells, CPAP/SAS-4 is required for the assembly of nine triplet centriolar MTs during the early stage of procentriole formation (Tang *et al*, 2009). However, less is known about how the cartwheel is connected to the MT triplets in human cells. To determine whether hSAS-6 or CEP135 could interact with MTs, we performed MT co-sedimentation assays *in vivo*. HEK 293T cells were lysed with BRB80 buffer and cell extracts were treated with or without the MT-stabilizing drug, Taxol. After treatment, cell extracts were centrifuged, separated into supernatant and pellet fractions, and analysed by IB. As shown in Figure 3B, the α-tubulin of MTs was clearly detected in the pellet fractions of Taxol-treated extracts. Interestingly, most of the endogenous CEP135 co-precipitated with MTs in the pellet fractions, whereas the hSAS-6 protein mainly stayed in the supernatant. These results indicate that CEP135, but not hSAS-6, is capable of binding MTs.

To determine the MT-binding region in CEP135, we transfected various CEP135-myc truncated fragments into HEK 293T cells and conducted MT co-sedimentation analyses. Our results showed that the N-terminal region of CEP135 (residues 1–415) efficiently co-precipitated with MTs *in vitro* (Figure 3C). To further narrow the MT-binding domain and investigate whether CEP135 could directly bind to MTs, we incubated two recombinant GST-CEP135 proteins, GST-CEP135 (residues 1–190) and GST-CEP135 (residues 190–415), with purified tubulin in the presence of Taxol, and performed *in vitro* MT co-sedimentation assays.

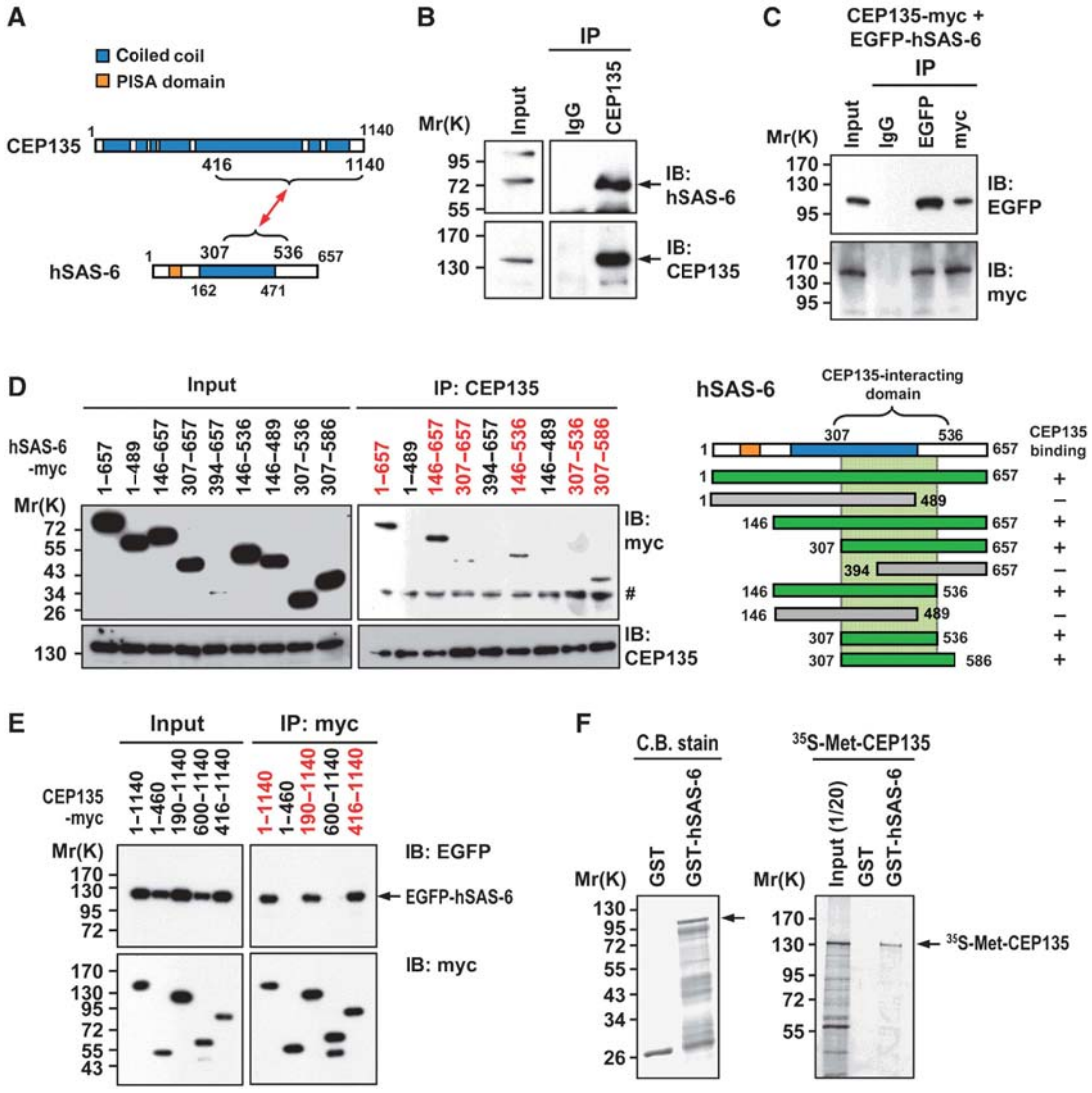

Figure 2 CEP135 directly interacts with hSAS-6. (**A**) A schematic showing the interacting regions of CEP135 and hSAS-6. (**B**) Endogenous CEP135 and hSAS-6 form a complex *in vivo*. Western blot analysis of immunoprecipitated (IP) complexes containing endogenous CEP135 and hSAS-6 prepared from HEK 293T cell lysates using an anti-CEP135 antibody and control IgG. (**C**) CEP135 interacts with hSAS-6 in transfected cells. HEK293T cells were co-transfected with CEP135-myc and EGFP-hSAS-6. Twenty-four hours after transfection, cell lysates were IP with anti-myc, anti-EGFP or IgG antibodies and then immunoblotted (IB) with the indicated antibodies. (**D**) Mapping the CEP135-interacting domain in hSAS-6. HEK293T cells were transfected with various myc-tagged hSAS-6 constructs and analysed by IP using an anti-CEP135 antibody. # indicates non-specific bands. (**E**) Mapping the hSAS-6-interacting domain in CEP135. HEK293T cells were co-transfected with a vector encoding full-length EGFP-hSAS-6 and various myc-tagged CEP135 constructs, and analysed by IP using an anti-myc antibody. (**F**) CEP135 directly interacts with hSAS-6. The full-length ^{35}S-methionine-labelled CEP135 proteins were incubated with bead-bound GST or GST-hSAS-6 and analysed by SDS–PAGE and autoradiography.

As shown in Figure 3D, the most N-terminal polypeptide (residues 1–190) of CEP135 revealed a strong interaction with MTs. Since no proteins other than purified GST recombinant proteins and tubulins were present in the reactions, we conclude that the N-terminus of CEP135 (residues 1–190) directly binds to MTs. Consistent with this finding, the N-terminus of *Drosophila* Bld10/CEP135 was also reported that directly interacts with MTs (Carvalho-Santos *et al*, 2012).

To further confirm this effect *in vivo*, We ectopically expressed myc-tagged CEP135 constructs (full-length CEP135 and CEP135-1–190) in U2OS cells and found that the overexpressed N-terminal CEP135 fragment (1–190; Figure 3E-i), but not the full-length CEP135 (Figure 3E-iii), bound to MTs in cells. However, the binding of CEP135 (1–190) to MTs was significantly disrupted in the presence of nocodazole (a MT-destabilizing drug), suggesting that nocodazole may destabilize the CEP135 (1–190)-bound MTs (Figure 3E-ii). Unexpectedly, overexpressed full-length human CEP135 formed aggregates in cells and appeared not to interact with cytoplasmic MTs (Figure 3E-iii). The reason for this is currently not known. One possibility is that the N-terminal-most domain (residues 1–190) that binds to MTs is folded and buried inside the intact CEP135 molecule, blocking its binding to MTs. Taken together, our results define the N-terminal 190 residues of CEP135 as directly binding to MTs.

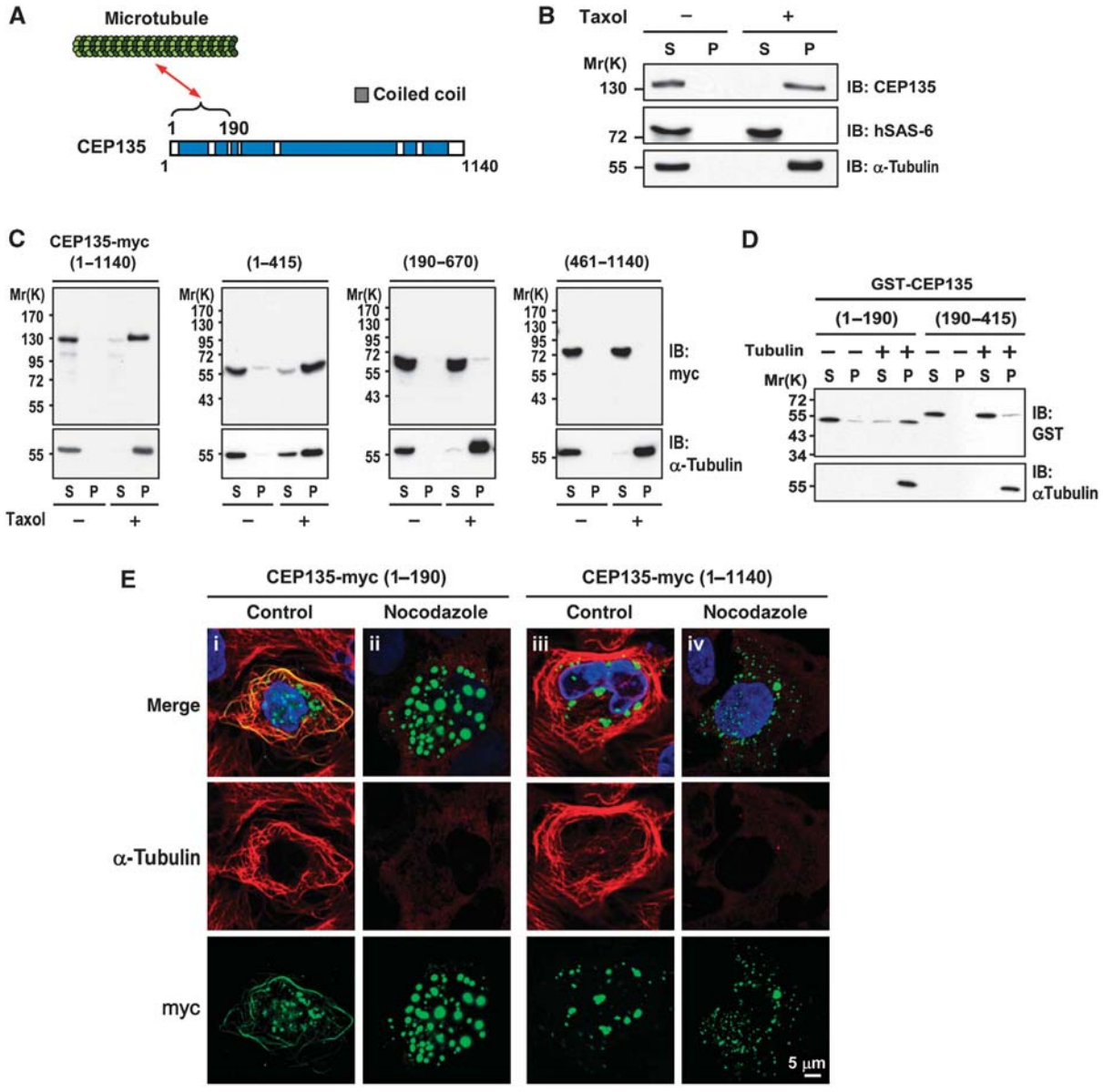

Figure 3 CEP135 directly binds to microtubules. (**A**) Schematic of the interaction between CEP135 and microtubules. (**B**) CEP135, but not hSAS-6, co-precipitates with microtubules. HEK293T cells were lysed in lysis buffer in the presence or absence of Taxol. The cell lysates were centrifuged, separated into supernatant (S) and pellet (P) fractions, and analysed by IB using the indicated antibodies. (**C**) Full-length and the N-terminal region of CEP135-myc (residues 1–415) co-precipitates with microtubules. HEK293T cells were transfected with various myc-tagged CEP135 truncation mutants. Twenty-four hours after transfection, cells were lysed and analysed as described in (**B**). (**D**) CEP135 directly binds to microtubules. Purified tubulins were incubated with the indicated GST-tagged recombinant CEP135 proteins in the presence of Taxol. The supernatant (S) and pellet (P) fractions were analysed by IB. (**E**) CEP135-myc (residues 1–190) binds to microtubules *in vivo,* and this MT binding is destabilized by nocodazole treatment. U2OS cells were transfected with CEP135-myc (1–190) or full-length CEP135 (1–1140). Twenty-four hours after transfection, cells were treated without (control) or with nocodazole (2.5 μM) for 1 h, and then analysed by immunofluorescence confocal microscopy using the indicated antibodies.

Depletion of CEP135 results in abnormal centriole structures with altered triplet numbers and shorter centrioles

The observations that CEP135 directly binds to MTs and is required for centriole duplication led us to hypothesize that CEP135 may play a role in the maintenance of proper MT walls in centrioles. Accordingly, we depleted CEP135 with siRNA-mediated knockdown in U2OS cells and analysed the centriolar structure by electron microscopy. As shown in Figure 4, CEP135-depleted cells appeared to have abnormal centriolar structures. From 17 centrioles acquired, 3 of 7 in transverse view had defective centrioles with abnormal numbers of triplets (5 triplets, Figure 4B-ii; 7 triplets, Figure 4B-iv) while the other 10 centrioles when viewed in longitudinal section are shorter than normal (WT = 0.414 ± 0.016 μm, Figure 4A-i; siCEP135 = 0.332 ± 0.017 μm; Figure 4B-iii). We also observed a severe defect at the distal end of outer centriolar MTs in a mother centriole (arrowhead in Figure 4B-i). Quantitative analysis of the centriole length in siControl and siCEP135-treated cells is shown in Figure 4C.

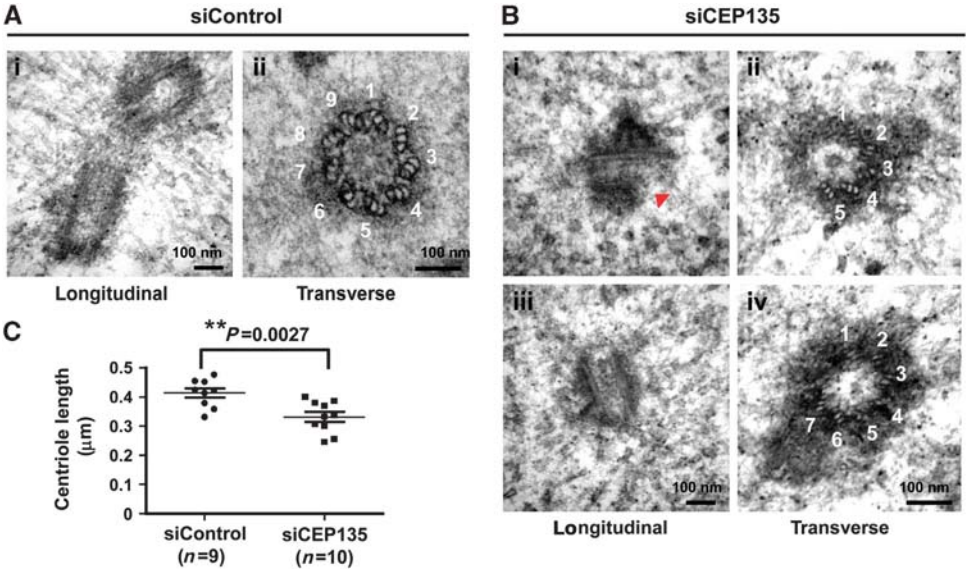

Figure 4 CEP135 is required to build a correct centriole structure and maintain the proper length of the human centriole. U2OS cells were treated with siControl (**A**) or siCEP135 (**B**) for 3 days, synchronized at G1/S by thymidine for another day, released from thymidine treatment for 5 h, and analysed by electron microscopy. (**B**) Depletion of CEP135 was associated with abnormal centriole structures and altered triplet numbers (5 triplets, **B**-ii and 7 triplets, **B**-iv). The red arrowhead indicates a defect at the distal end of outer centriolar MTs (**B**-i). CEP135 depletion also caused shorter centrioles (**B**-i and **B**-iii). (**C**) Quantitative analysis of centriole length acquired by EM images in siControl ($n = 9$) and siCEP135 ($n = 10$) treated cells.

Together, our results suggest that CEP135 is required to build a correct centriole structure and maintain the proper length of the human centriole.

CEP135 depletion appears to have little or no effect on the recruitment of hSAS-6 to the centriole

As our above results indicated that CEP135 directly interacts with hSAS-6 and maintains the proper structure of the nine-fold symmetry, we next examined whether the centriolar localization of hSAS-6 was dependent on CEP135 and vice versa. U2OS-based EGFP-centrin-expressing cells or U2OS cells were transfected with hSAS-6- or CEP135-targeting siRNAs, and the cells were synchronized at early S phase by aphidicolin treatment. Immunofluorescent analysis revealed a very weak decrease in the centriolar hSAS-6 signals in CEP135-depleted cells (Supplementary Figure S2A and B), implying that the recruitment of hSAS-6 to the centriole is probably not dependent on CEP135. We next examined whether hSAS-6 depletion affects CEP135 targeting to the centrioles. As shown in Supplementary Figure S2C and D, depletion of hSAS-6 did not appear to affect the centriolar localization of CEP135. Because CEP135 was reported to be localized at the proximal lumen of both parental centrioles and procentrioles (Kleylein-Sohn *et al*, 2007), it was difficult to distinguish the newly recruited CEP135 from the pre-existing CEP135 on the parental centrioles by immunofluorescence staining. We thus suggest that the recruitment of hSAS-6 to the cartwheel structure might be CEP135 independent, but vice versa is not clear.

A CEP135 mutant that lacks the proper interaction with hSAS-6 perturbs centriole duplication

Since we found that the C-terminus of CEP135 (residues 416–1140) directly binds to hSAS-6 (Figure 2), we next examined whether intrinsic hSAS-6-binding activity is required for the function of CEP135 in centriole duplication. We generated a proline mutant (L588P, Figure 5A) that disrupted the predicted α-helical structures of the conserved C-terminal coiled-coil regions (Figure 5A). We then co-transfected full-length CEP135-myc (wild-type and L588P mutant) plus EGFP-hSAS-6 into HEK293T cells, and subjected cell lysates to co-IP assays (Figure 5B). Our results showed that the CEP135-myc mutant (L588P) showed greatly reduced binding to hSAS-6 (Figure 5B). The specific disruption of the interaction between the L588P mutant and hSAS-6 was further confirmed by a yeast two-hybrid assay (Figure 5C). Interestingly, overexpression of the CEP135-myc (L588P) mutant appeared to interfere with centriole duplication (Figure 5D), but not the centriolar localization of itself (Figure 5E) or hSAS-6 (Figure 5F). Collectively, we conclude that the intrinsic hSAS-6-binding activity of CEP135 is critical for centriole duplication, but not for the recruitment of hSAS-6 to the cartwheel.

CEP135 is required for both PLK4- and STIL-mediated centriole amplification

PLK4 is a key player in the onset of centriole duplication in human cells (Habedanck *et al*, 2005; Kleylein-Sohn *et al*, 2007). To examine the role of CEP135 in the PLK4-mediated pathway, we depleted CEP135 in PLK4-overexpressing cells. Consistent with previous finding (Kleylein-Sohn *et al*, 2007), PLK4-mediated centriole amplification (>4 centrioles) was significantly inhibited in CEP135-depleted cells, and this inhibition could be effectively rescued by transfection with a CEP135 siRNA-resistant construct (Supplementary Figure S3). Thus, CEP135 is required for PLK4-mediated centriole amplification.

The human microcephaly protein, STIL (MCPH7), is a functional homologue of *Drosophila* Ana2 and *C. elegans* SAS-5. We previously showed that STIL overexpression

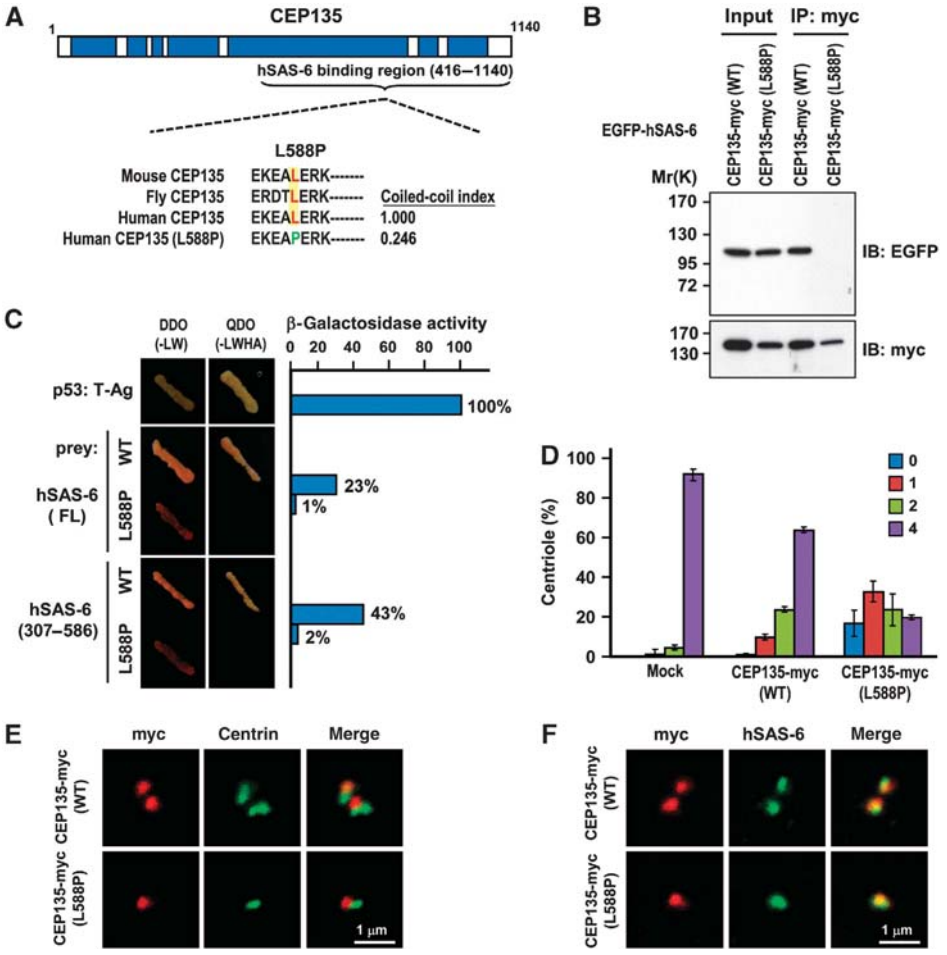

Figure 5 A CEP135 (L588P) mutant lacking the proper interaction with hSAS-6 shows perturbed centriole duplication. (**A**) Sequence alignment and summary of the CEP135 (L588P) mutant and its calculated coiled-coil index for forming an α-helical coiled-coil structure. Co-immunoprecipitation (**B**) and yeast two-hybrid experiments (**C**) revealed that the CEP135 (L588P) mutant had decreased binding to hSAS-6. In the yeast two-hybrid assay, a positive interaction was evidenced by the growth of mating colonies on QDO plates and the activation of β-galactosidase activity. CEP135 (residues 416–1140) was used as a bait. As positive controls, we used p53 (bait) and SV40-large T-Ag (prey). Overexpression of the CEP135 (L588P) mutant inhibits centriole duplication (**D**, **E**), but does not appear to interfere with the centriolar localization of CEP135 (**E**) or hSAS-6 (**F**). U2OS cells were treated with siCEP135 and transfected with vectors expressing full-length CEP135-myc wild-type or CEP135-myc L588P mutant. Forty-eight hours after transfection, the cells were analysed by immunofluorescent confocal microscopy using the indicated antibodies (**E**, **F**). Bar values are means ± s.d ($n = 100$ cells) of three independent experiments (**D**).

induced centriole amplification, while its depletion significantly inhibited PLK4-induced centriole amplification (Tang *et al*, 2011). To examine whether CEP135 is also required for STIL-mediated centriole amplification, we depleted CEP135 from U2OS cells that ectopically expressed EGFP-STIL under tetracycline-mediated induction. As shown in Figure 6, it appears that CEP135 depletion not only inhibited EGFP-STIL-mediated centriole amplification (Figure 6A and D), but also perturbed the localization of EGFP-STIL to the centrioles (Figure 6A and E). Most siCEP135-depleted cells contain either one (∼38%) or two centrioles (∼47%) (Figure 6D). Together, our results suggest that CEP135 is essential for STIL-mediated centriole duplication.

CEP135 is required for the centriolar localization of CPAP and CEP135 depletion inhibits CPAP-induced centriole elongation

We (Tang *et al*, 2009) and others (Kohlmaier *et al*, 2009; Schmidt *et al*, 2009) previously showed that excess CPAP can induce the formation of extra long centrioles. In the present study, we found that CEP135 directly interacts with hSAS-6 (Figure 2) and MTs (Figure 3), and maintains the proper structure of the nine triplets (Figure 4). Thus, we next examined whether CEP135 is required for CPAP-induced centriole elongation. We depleted CEP135 from CPAP-myc-inducible cells using the protocol described in Figure 7H. Our immunofluorescent results revealed that CEP135 partially co-localized with CPAP-myc and Ac-tubulin-labelled filaments in siControl cells (Figure 7A). Upon depletion of CEP135, however, the centriolar staining of CPAP-myc (Figure 7A and B) and the centriole length (Figure 7C) decreased significantly compared with siControl cells. Importantly, we observed that the number of elongated centrioles induced by excess CPAP-myc was severely impaired in CEP135-depleted cells (∼23% in siCEP135 versus 49% in siControl; Figure 7D). This could be effectively rescued by exogenously expression of a CEP135 RNAi-resistant construct (EGFP-CEP135-R; Figure 7D and F), indicating that this was a specific effect of CEP135 depletion. Intriguingly, most of the CEP135-depleted cells contained either a single mature parent centriole (ODF2-positive,

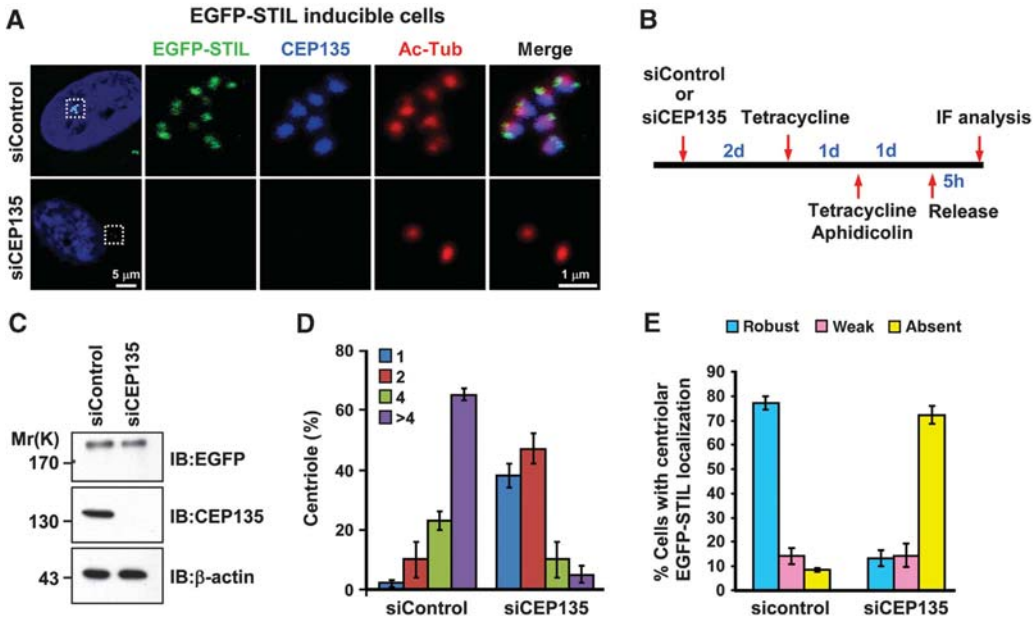

Figure 6 CEP135 depletion not only inhibits EGFP-STIL-induced centriole amplification but also perturbs EGFP-STIL targeting to the centrioles. U2OS-based EGFP-STIL-inducible cells were treated with siControl or siCEP135 as described in (**B**). Because STIL is absent from G1 cells, EGFP-STIL inducible cells were synchronized at S phase to ensure the detection of EGFP-STIL after siCEP135 treatment. The cells were then analysed by immunofluorescent confocal microscopy (**A**) or immunoblotting (**C**) using the indicated antibodies. EGFP-STIL was directly visualized by a fluorescent confocal microscope. (**D**) Histogram illustrating the percentages of cells showing centriole numbers ($n = 100$ in triplicate). (**E**) Quantitative analysis of the relative centriolar intensity of EGFP-STIL in siCEP135-treated cells ($n = 100$ in triplicate).

40%; Figure 7G-i) or one short ODF2-positive centriole (parent centriole) and one short ODF2-negative centriole (daughter centriole) (37%, Figure 7G-ii), suggesting that CEP135 knockdown affects CPAP-induced centriole elongation from both centrioles.

CEP135 directly interacts CPAP and forms a complex with hSAS-6

We next examined whether CEP135 could possibly interact and form a complex with CPAP. A myc-tagged CEP135 construct was transiently transfected into HEK 293T cells, and cell lysates were analysed by IP with an anti-CPAP antibody. As shown in Figure 8B, both CEP135 and hSAS-6 were detected in the CPAP immunoprecipitates, implying that these three proteins may possibly form an interacting complex *in vivo*. The hSAS-6-CEP135-CPAP protein complex has also been independently demonstrated by a pull-down assay using a full-length GST-hSAS-6 recombinant protein (Supplementary Figure S4A).

To investigate whether CEP135 could interact with CPAP, HEK293T cells were transfected with a series of myc-tagged CEP135 truncation constructs, and IP experiments were performed using an anti-CPAP antibody. Our results showed that the N-terminal polypeptide of CEP135 (residues 50–460) could be co-precipitated with CPAP (Figure 8C). Further GST pull-down experiments demonstrate that only GST-CEP135 (residues 1–460) could specifically pull-down ^{35}S-methionine-labelled full-length CPAP (Supplementary Figure S4B), indicating a direct interaction between these two proteins.

Using similar approaches, we mapped the CEP135-interacting domain to the C-terminal region of CPAP (Figure 8D). Our co-IP experiments showed that the GFP-tagged C-terminal region of CPAP (residues 895–1338) could be co-precipitated with endogenous CEP135 (Figure 8D). Further studies demonstrated that GST-CPAP (895–1338) can directly interact not only with ^{35}S-methionine-labelled full-length CEP135 (Supplementary Figure S4D), but also with His-tagged CEP135 (residues 1–460) recombinant protein (Supplementary Figure S4C). A schematic of the interaction between CEP135 and CPAP is shown in Figure 8A. In addition, we used GST pull-down assays to demonstrate that recombinant GST-CPAP (895–1388) could pull down a complex containing endogenous hSAS-6 and CEP135 (Supplementary Figure S4A). This is consistent with the notion that all three molecules (hSAS-6, CEP135, and CPAP) may form a complex in cells.

Our co-IP experiments (Figure 8C) suggested that two short regions (residues 50–190 and 415–460) in the N-terminal domain of CEP135 appear to be essential for binding with CPAP, as truncated CEP135 fragments lacking either region lost their ability to bind CPAP. Intriguingly, the most N-terminal domain (residues 1–190) of CEP135 also binds to MTs (Figure 3). In the future, it will be interesting to determine how CEP135 interacts with CPAP to promote centriolar MT assembly. Taken all together, our results support the notion that CEP135 may directly interact with CPAP to the centriole and is required for CPAP-induced centriole elongation. Thus, the formation of a proper 'cartwheel' structure that contains hSAS-6 and CEP135 appears to be an essential prerequisite for CPAP-mediated MT assembly during centriole elongation.

Discussion

Centrioles are composed of nine triplets of MTs organized around a cartwheel structure, which is highly conserved among various eukaryotic organisms (Figure 9A, reviewed by Azimzadeh and Marshall, 2010 and Gonczy, 2012). In most

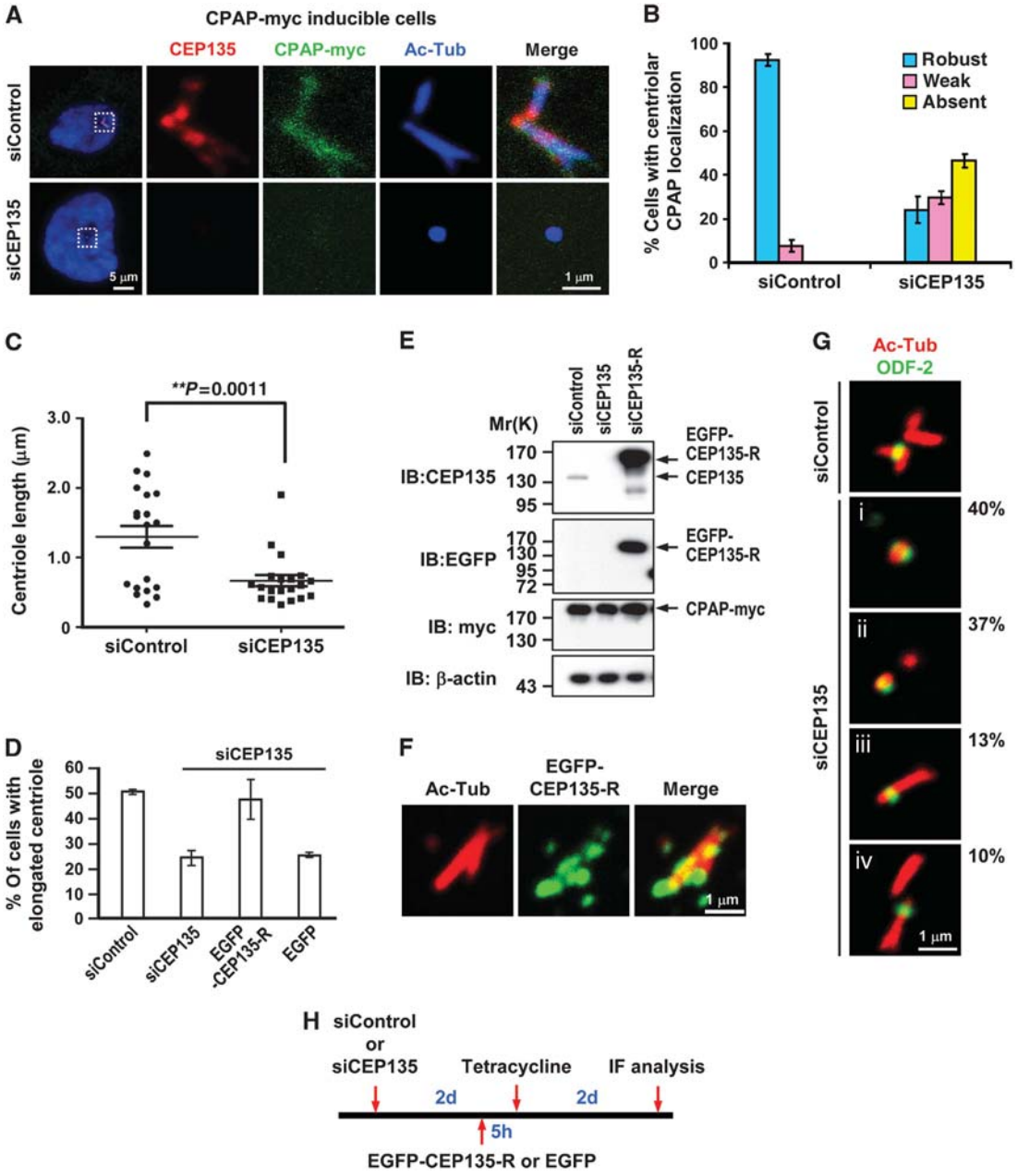

Figure 7 Depletion of CEP135 impairs the recruitment of CPAP to the centriole and inhibits CPAP-induced centriole elongation. (**A**) CPAP-myc-inducible cells were transfected with siControl or siCEP135 for 2 days, followed by tetracycline induction for another 2 days and analysis by immunofluorescent confocal microscopy using the indicated antibodies. (**B**) Quantitative analysis of the relative centriolar intensity of CPAP-myc in siRNA-treated cells. (**C**) Quantitative analysis of the elongated centrioles induced by CPAP-myc overexpression in siControl- and siCEP135-treated cells. Bar values are means ± s.d of three independent experiments; $P = 0.0011$. (**D**) Histogram illustrating the percentages of cells showing elongated centrioles (counted by Ac-tubulin; $n = 100$ in triplicate). In siRNA rescue experiments (**D**–**F**), CPAP-myc-inducible cells were transfected with siCEP135, followed by transfection of a vector encoding siRNA-resistant EGFP-CEP135-R or EGFP, tetracycline induction as shown in (**H**). The cells were then analysed by IB (**E**) and immunofluorescent staining (**F**) using the indicated antibodies. Elongated centrioles were effectively rescued by the expression of EGFP-CEP135 in siCEP135-treated cells (**D**, **F**). (**G**) CEP135 depletion inhibits CPAP-induced centriole elongation.

vertebrate cells, each triplet contains an A-microtubule, which is assembled first during centriole assembly and is the only complete MT with 13 protofilaments. The B- and C-microtubules are incomplete MTs that are assembled later. A recent study using cryo-electron microscopy showed that the proximal end of the A-microtubule in a nascent human procentriole is capped by a structure similar to the γ-tubulin ring complex (Guichard *et al*, 2010), a known MT nucleator in animal cells. In contrast, the incomplete B- and C-microtubules are never capped at their proximal ends, and their appears to undergo bidirectional growth along the A- or B-microtubules, respectively (Guichard *et al*, 2010).

The cartwheel has a central hub with nine spokes that connect with the A-microtubule through a pinhead. SAS-6 contains a relatively conserved N-terminal domain, followed by a coiled-coil domain and an unstructured C-terminal

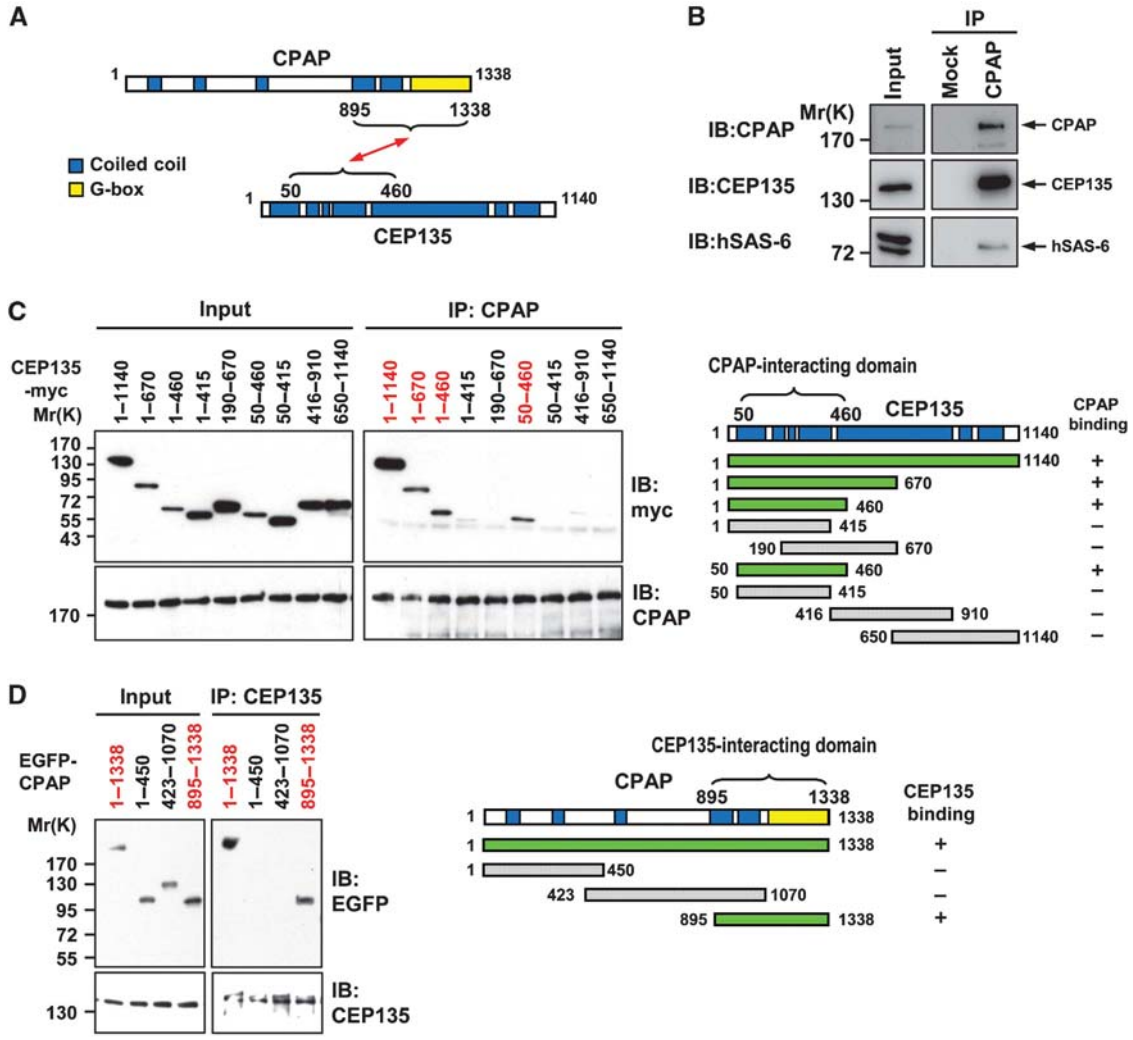

Figure 8 CEP135 directly interacts with CPAP and forms a complex with hSAS-6. (**A**) Schematic of interactions between CPAP and CEP135. (**B**) IB analysis of IP complexes from HEK293T cells expressing CEP135-myc. After transfection, the cell lysates were IP with an anti-CPAP antibody or an irrelevant normal IgG (Mock) and analysed by IB using the indicated antibodies. (**C**) Mapping the CPAP-interacting domain in CEP135. HEK293T cells were transfected with various myc-tagged CEP135 constructs and analysed by IP using an anti-CPAP antibody. (**D**) Mapping the CEP135-interacting domain in CPAP. HEK293T cells were transfected with various EFGP-tagged CPAP constructs and analysed by IP using an anti-CEP135 antibody.

domain. X-ray crystallographic analysis was used to propose a structural model of the SAS-6-based cartwheel (Kitagawa *et al*, 2011; van Breugel *et al*, 2011), wherein the N-terminal domain of SAS-6 self-assembles into a ring similar to the central hub, while the middle coiled-coil domain contributes to form the spokes. Intriguingly, *C. reinhardtii* Bld10, an orthologue of human CEP135, was reported to be localized at the pinhead region of the cartwheel (Matsuura *et al*, 2004; Hiraki *et al*, 2007). However, it was not previously known whether Bld10/CEP135 functions to physically connect the cartwheel spokes to the peripheral MT triplets in human cells. In the present study, we provide evidence to show that CEP135 acts as a bridging molecule that directly binds to hSAS-6 through its carboxyl terminus (Figure 2) and MTs via its amino terminus (Figure 3). This CEP135-mediated connection seems to be essential to stabilize the cartwheel structure and is required for CPAP-mediated centriole elongation. Importantly, we herein propose the first detailed molecular mechanism for the function of CEP135 in centriole duplication in human cells.

What is the physiological role of human microcephaly protein CEP135 at the onset of procentriole formation? A proposed model is depicted in Figure 9. One possible scenario is that CEP135 directly binds to a region close to the C-terminus of hSAS-6, and this interaction is essential for cartwheel stabilization and procentriole formation. This notion is supported by previous reports showing that the C-terminus of *Chlamydomonas* SAS-6 is located at the distal region of the centriolar cartwheel spoke (van Breugel *et al*, 2011), where the Bld10 is also localized (Hiraki *et al*, 2007). Furthermore, our present observations show that a CEP135 mutation (L588P) that disrupted its interaction with hSAS-6 inhibited centriole duplication (Figure 5D), and depletion of CEP135 not only led to the development of abnormal centriole structures (Figure 4), but also blocked PLK4- (Supplementary Figure S3) and STIL-mediated centriole amplification (Figure 6) are also consistent with this model.

On the other hand, CEP135 may directly bind to CPAP and a 'short segment' of an MT (possibly A-microtubule) that was

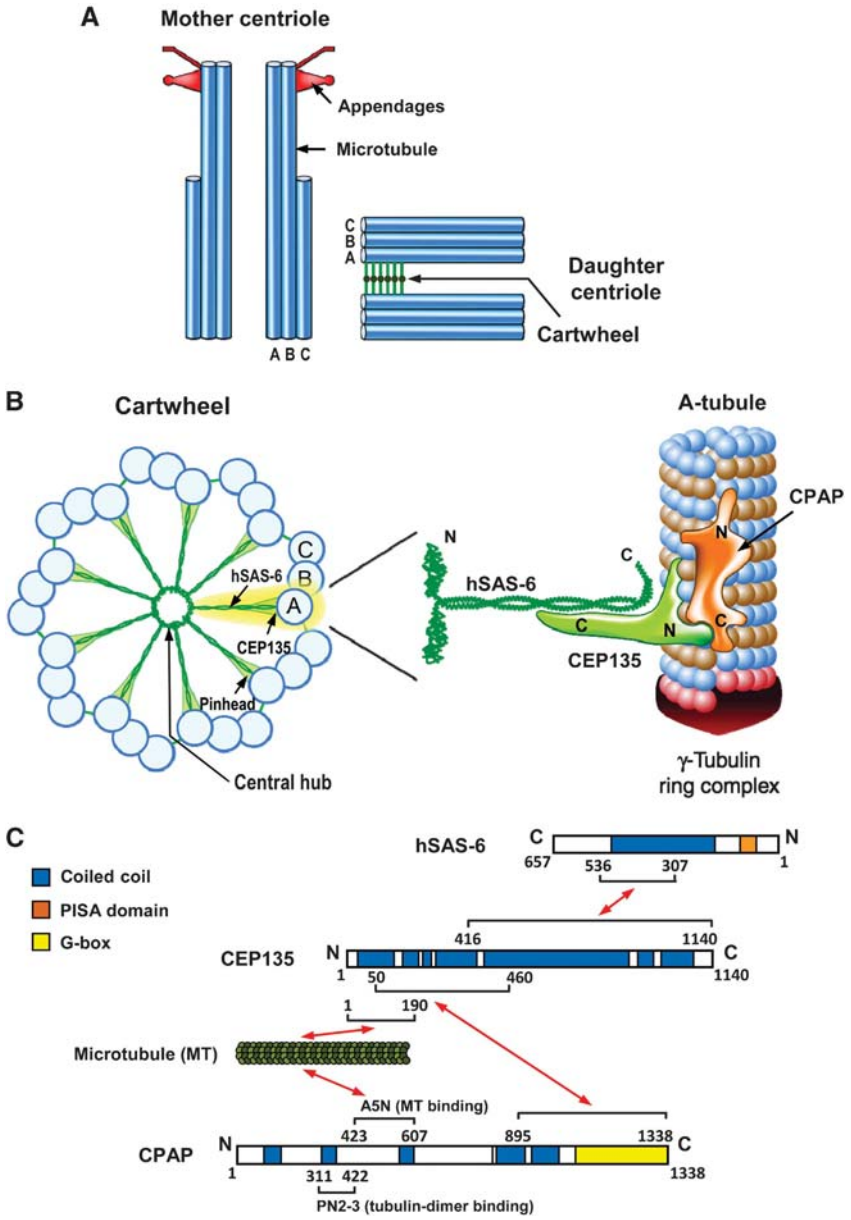

Figure 9 A proposed model for how CEP135 stabilizes the cartwheel structure and is required for CPAP-mediated centriole elongation. (**A**) Schematic representation of mother and daughter centriole pair in a human cell. (**B**) Schematic representation of the cartwheel and its associated proteins viewed from the proximal end (left). A close-up view of the A-tubule and its associated proteins (right) is enlarged and rotated 90° from the view on the left (A-tubule). CEP135 in the pinhead serves as a bridging protein that directly interacts with hSAS-6 in the central hub via its C-terminal region, and with the outer microtubules (possibly the A-tubule) and CPAP through its N terminus. CPAP carries both a tubulin dimer-binding domain (PN2-3) (Hung *et al*, 2004) and a microtubule-binding domain (A5N) (Hsu *et al*, 2008), and is associated with the γ-tubulin complex (Hung *et al*, 2000). The CPAP C-terminus directly interacts with the CEP135 N-terminus and promotes centriolar microtubule assembly. The A-tubule, which contains 13 protofilaments and is end-capped by the γ-tubulin ring complex (Guichard *et al*, 2010), may be initiated by CPAP-trigged γ-tubulin-dependent nucleation occurring via a yet-unknown mechanism. (**C**) Schematic summary of the established interactions of hSAS-6, CEP135, microtubules, and CPAP, and their corresponding structural and functional domains.

possibly pre-formed by an unknown process of CPAP-trigged γ-tubulin-dependent nucleation (Azimzadeh and Marshall, 2010; this report). In agreement with this hypothesis, cryo-electron tomography revealed that the proximal end of the A-microtubule is capped by a conical structure resembling the γ-TuRC (Guichard *et al*, 2010) and CPAP was reported to be associated with the γ-tubulin complex (Hung *et al*, 2000). Furthermore, CEP135 appears to be required for CPAP-mediated centriole elongation at the later stage of procentriole assembly. Depletion of CEP135 not only blocked CPAP-induced centriole elongation, but also greatly perturbed the recruitment of CPAP to the centriole (Figure 7A and B), implying that CEP135 is essential for CPAP-mediated centriolar MT assembly.

It is interesting to note that CPAP may also directly interact with STIL and indirectly form a complex with hSAS-6 (Tang *et al*, 2011). How are these two complexes (hSAS-6/CEP135/CPAP and hSAS-6/STIL/CPAP) with overlapping components related to each other? There are two possibilities. First, at least two CPAP-containing complexes are present in the cytosol, each of which may play a role at different hierarchical levels during procentriole formation. Another

possibility is that at least four proteins (i.e., STIL, CPAP, CEP135, hSAS-6, and possibly others) form a complex within the cells. These two possibilities may not be mutually exclusive. Currently, we do not yet understand the spatio-temporal regulation of these CPAP-containing complexes during procentriole formation. Future biochemical and functional characterizations of these CPAP-containing complexes may resolve this puzzle.

In addition to suggesting that CEP135 links the central hub protein, hSAS-6, to the outer MTs, our study demonstrated that CEP135 depletion produced shorter centrioles (Figure 4C). Similar results were also observed in siBld10-treated *Paramecium* (Jerka-Dziadosz *et al*, 2010) and in *Drosophila bld10*/CEP135 mutants (Mottier-Pavie and Megraw, 2009). Together, these findings suggest that CEP135 may have a second function: that of maintaining proper centriole lengths in human cells.

Finally, a C-terminally deleted CEP135 mutant was reported to cause primary microcephaly with disturbed centrosomal function in patient fibroblasts (Hussain *et al*, 2012). Our present findings offer a possible molecular explanation for such a defect in humans. It is possible that a C-terminally truncated CEP135 mutant lacking the hSAS-6-interacting region may destabilize the SAS-6-based cartwheel structure possibly by disrupting the interaction between CEP135, hSAS-6, and A-microtubules. This could result in defective triggering of CPAP-mediated centriole elongation at a later stage. It will be interesting to examine the integrity of the CEP135-hSAS-6 complex in these patients. Furthermore, recent studies have shown that mutations in *CEP152* (MCPH4) (Guernsey *et al*, 2010; Kalay *et al*, 2011), *CPAP/CENPJ* (MCPH 6) (Bond *et al*, 2005), *STIL* (MCPH 7) (Kumar *et al*, 2009), *CEP135* (MCPH 8) (Hussain *et al*, 2012), and *CEP63* (Sir *et al*, 2011) cause primary microcephaly in humans, and direct interactions among these proteins, including CEP63-CEP152 (Sir *et al*, 2011), CEP152-CPAP (Cizmecioglu *et al*, 2010; Dzhindzhev *et al*, 2010), STIL-CPAP (Tang *et al*, 2011; Vulprecht *et al*, 2012), and CPAP-CEP135-hSAS-6 (this report), appear to participate at the onset of procentriole formation. These findings strongly support the notion that defective centriole duplication, possibly due to inhibited production of intact functional centrioles in neuronal progenitor cells, may be a major cause of MCPH in human patients.

Materials and methods

Plasmids and antibodies

The cDNA encoding full-length CEP135 was obtained by RT–PCR from total RNA of human HEK 293T cells and subcloned in-frame into pEGFP-C1 (BD Biosciences Clontech) or pcDNA4/TO/Myc–His-A (Invitrogen). To generate the siRNA-resistant CEP135 construct, the siRNA-targeted nucleotides within wild-type CEP135 were partially replaced without changing the amino-acid sequence using a QuikChange kit (Stratagene). To construct the GST-fusion plasmids, cDNAs encoding various portions of CEP135 were fused in-frame to GST in pGEX-2T or pGEX-4T vector as described previously (Tang *et al*, 2009). The rabbit polyclonal antibody against CEP135 was raised using recombinant CEP135-His (residues 650–1140), and affinity purified. The antibodies against CPAP (1:1000 dilution), hSAS-6 (1:500 dilution), and centrin 2 (1:500 dilution) were as previously described (Tang *et al*, 2009). Other commercially available antibodies used in this study included anti-SAS-6 mAb (Abnova); anti-ODF2 (Abcam), anti-β-actin, anti-α-tubulin, anti-γ-tubulin, and anti-acetylated tubulin (all from Sigma-Aldrich); anti-myc (4A6, Upstate Biotechnology or NB600-336, Novus Biologicals, Inc); and anti-GFP (BD Bioscience).

Cell culture and synchronization

U2OS and HEK 293T cells were maintained in Dulbecco's modified Eagle's medium supplemented with fetal bovine serum (10%). The tetracycline-inducible CPAP-myc and EGFP-STIL lines were as described previously (Tang *et al*, 2009, 2011), and the expression of CPAP-myc and EGFP-STIL was induced with 1 μg/ml tetracycline. U2OS-based lines stably expressing GFP-centrin were as described previously (Tang *et al*, 2011). For synchronization experiments, cells were arrested at early S phase by incubation with aphidicolin (2 μg/ml) for 24 h, as previously described (Tang *et al*, 2011).

Transfection and siRNA experiments

Cells were transiently transfected with various cDNA constructs using Lipofectamine 2000, as previously described (Tang *et al*, 2011). The siRNAs against hSAS-6 and CPAP were as described previously (Tang *et al*, 2011), and those against CEP135 (siCEP135-1 and siCEP135-2) are listed below. These siRNAs and a non-targeting siRNA control were purchased from Invitrogen, and transfections were performed using RNAiMAX (Invitrogen). Because CEP135 is a stable protein and reveals a strong staining within the proximal lumen of both parental centrioles and procentrioles (Kleylein-Sohn *et al*, 2007), we commonly treated the cells with high-dose siRNAs (66 nM) and long incubation time (~4 days).

siCEP135-1: 5′-UUUACAAGGAGUUCAUCACUCAGUC-3′
siCEP135-2: 5′-AUAACUUGUAGAGCAAGAUCUUCGC-3′.

Immunoprecipitation, GST pull-down assay, and yeast two-hybrid assay

HEK 293T cells were transiently transfected with various constructs. Twenty-four hours after transfection, the cells were lysed in RIPA buffer (50 mM Tris–HCl at pH 8.0, 150 mM NaCl, 1% NP-40, 0.5% sodium deoxycholate, 20 mM β-glycerophosphate, 20 mM NaF, 1 mM Na_3VO_4, and protease inhibitors including 1 mg/ml leupeptin, 1 mg/ml pepstatin and 1 mg/ml aprotinin). In some experiments (e.g., Figure 8B), we used a less stringent lysis buffer (RIPA buffer without 0.5% sodium deoxycholate) to lyse the cells. The cell lysates were subjected to IP with the indicated antibodies for 2 h at 4°C and then incubated with protein-G-sepharose beads for another 2 h. For immunoblot analysis, the immunoprecipitated complexes were separated by SDS–PAGE and probed with the appropriate antibodies.

To examine the direct interaction between CEP135 and hSAS-6 or the interaction between CEP135 and CPAP, full-length recombinant GST-hSAS-6 or various GST-CEP135 truncated recombinant proteins were used to pull down full-length ^{35}S-methionine-labelled CEP135 or CPAP proteins, respectively, that had been generated by *in vitro* transcription-translation using the TNT T7 Quick Coupled Transcription/Translation System (Promega). GST was used as a negative control. After binding, the beads were boiled in sample buffer and analysed by autoradiography, as previously described (Tang *et al*, 2011).

Yeast two-hybrid analysis was used to demonstrate the direct interaction between CEP135 and hSAS-6, and was performed using the Matchmaker Gold yeast two-hybrid system (Clontech) as previously described (Tang *et al*, 2011).

Immunofluorescent confocal microscopy and electron microscopy

Cells on coverslips were cold-treated and fixed in methanol as described previously (Tang *et al*, 2011). The fixed cells were blocked with 3% BSA (Sigma-Aldrich) and incubated with the indicated primary antibodies. After washing, the cells were incubated with Alexa 488-, Alexa 568-, or Alexa 647-conjugated secondary antibodies (1:400 dilution, Invitrogen), as described previously (Tang *et al*, 2011). DNA was counterstained with DAPI (4, 6-diamidino-2-phenylindole). The samples were visualized using a LSM 510 META confocal system with a Plan Apochromat ×100 1.4 NA oil immersion objective. Images were acquired with AimImage Browser and ZEN software (Carl Ziess, Inc.). We commonly used an affinity purified anti-CEP135 antibody (1:1000 dilution) for immunofluorescent staining experiments.

Furthermore, due to the absence of STIL and hSAS-6 in G1 cells, in some experiments, cells were synchronized by aphidicolin or thymidine treatment to ensure the detection of STIL and hSAS-6 at early S phase.

For electron microscopy, cells were fixed in glutaraldehyde (2.5%) for 1 h, washed three times with PBS buffer, post-fixed in osmium tetroxide (2%) for 1 h, dehydrated with serial ethanol, and embedded in LR white resin. Thin sections (70 nm) were placed on grids, stained with uranyl acetate and lead citrate, and examined with a transmission electron microscope (H7000, Hitachi Company).

In vitro and in vivo MTco-sedimentation assays

For *in vitro* MT co-sedimentation assays, purified tubulin (2.5 mM) was incubated with various truncated GST-CEP135 proteins in BRB80 buffer (80 mM PIPES pH 6.9 and 1 mM $MgCl_2$) containing 20 μM Taxol, 1 mM GTP and 1 mM DTT for 30 min at 30°C. After incubation, samples were centrifuged at 100 000*g* for 20 min at 30°C, and then analysed by western blotting. For *in vivo* MT co-sedimentation assays, HEK 293T cells were transfected with myc-tagged CEP135 plasmids. Twenty-four hours after transfection, the cells were harvested and lysed in BRB80 buffer with 0.1% NP-40. After centrifugation, the supernatant was incubated with a solution containing 20 μM Taxol, 1 mM GTP and 1 mM DTT for 15 min at 30°C. After incubation, the reaction mixtures were then layered on a cushion buffer (BRB80 buffer with 40% sucrose and 20 μM Taxol) and centrifuged at 100 000*g* for 15 min at 30°C. After centrifugation, the samples were boiled in sample buffer, separated by SDS–PAGE, and analysed by western blotting.

Supplementary data

Supplementary data are available at *The EMBO Journal* Online (http://www.embojournal.org).

Acknowledgements

This work was supported by a grant (NSC 100-2311-B-001-012-MY3) from the National Science Council, ROC, and from Academia Sinica Investigator Award.

Author contributions: Y-CL and C-WC performed and designed the experiments, and analysed the data; W-BH, C-JCT, Y-NL, E-JC, and C-TW performed experiments. TKT conceived and supervised the project, and wrote the paper.

Conflict of interest

The authors declare that they have no conflict of interest.

References

Arquint C, Sonnen KF, Stierhof YD, Nigg EA (2012) Cell-cycle-regulated expression of STIL controls centriole number in human cells. *J Cell Sci* **125:** 1342–1352

Azimzadeh J, Hergert P, Delouvee A, Euteneuer U, Formstecher E, Khodjakov A, Bornens M (2009) hPOC5 is a centrin-binding protein required for assembly of full-length centrioles. *J Cell Biol* **185:** 101–114

Azimzadeh J, Marshall WF (2010) Building the centriole. *Curr Biol* **20:** 816–825

Bettencourt-Dias M, Hildebrandt F, Pellman D, Woods G, Godinho SA (2011) Centrosomes and cilia in human disease. *Trends Genet* **27:** 307–315

Bettencourt-Dias M, Rodrigues-Martins A, Carpenter L, Riparbelli M, Lehmann L, Gatt MK, Carmo N, Balloux F, Callaini G, Glover DM (2005) SAK/PLK4 is required for centriole duplication and flagella development. *Curr Biol* **15:** 2199–2207

Bond J, Roberts E, Springell K, Lizarraga SB, Scott S, Higgins J, Hampshire DJ, Morrison EE, Leal GF, Silva EO, Costa SM, Baralle D, Raponi M, Karbani G, Rashid Y, Jafri H, Bennett C, Corry P, Walsh CA, Woods CG (2005) A centrosomal mechanism involving CDK5RAP2 and CENPJ controls brain size. *Nat Genet* **37:** 353–355

Brito DA, Gouveia SM, Bettencourt-Dias M (2012) Deconstructing the centriole: structure and number control. *Curr Opin Cell Biol* **24:** 4–13

Carvalho-Santos Z, Machado P, Alvarez-Martins I, Gouveia SM, Jana SC, Duarte P, Amado T, Branco P, Freitas MC, Silva ST, Antony C, Bandeiras TM, Bettencourt-Dias M (2012) BLD10/CEP135 is a microtubule-associated protein that controls the formation of the flagellum central microtubule pair. *Dev Cell* **23:** 412–424

Cizmecioglu O, Arnold M, Bahtz R, Settele F, Ehret L, Haselmann-Weiss U, Antony C, Hoffmann I (2010) Cep152 acts as a scaffold for recruitment of Plk4 and CPAP to the centrosome. *J Cell Biol* **191:** 731–739

Delattre M, Canard C, Gonczy P (2006) Sequential protein recruitment in C. elegans centriole formation. *Curr Biol* **16:** 1844–1849

Dobbelaere J, Josue F, Suijkerbuijk S, Baum B, Tapon N, Raff J (2008) A genome-wide RNAi screen to dissect centriole duplication and centrosome maturation in Drosophila. *PLoS Biol* **6:** e224

Dzhindzhev NS, Yu QD, Weiskopf K, Tzolovsky G, Cunha-Ferreira I, Riparbelli M, Rodrigues-Martins A, Bettencourt-Dias M, Callaini G, Glover DM (2010) Asterless is a scaffold for the onset of centriole assembly. *Nature* **467:** 714–718

Gonczy P (2012) Towards a molecular architecture of centriole assembly. *Nat Rev Mol Cell Biol* **13:** 425–435

Guernsey DL, Jiang H, Hussin J, Arnold M, Bouyakdan K, Perry S, Babineau-Sturk T, Beis J, Dumas N, Evans SC, Ferguson M, Matsuoka M, Macgillivray C, Nightingale M, Patry L, Rideout AL, Thomas A, Orr A, Hoffmann I, Michaud JL *et al* (2010) Mutations in centrosomal protein CEP152 in primary microcephaly families linked to MCPH4. *Am J Hum Genet* **87:** 40–51

Guichard P, Chretien D, Marco S, Tassin AM (2010) Procentriole assembly revealed by cryo-electron tomography. *EMBO J* **29:** 1565–1572

Habedanck R, Stierhof YD, Wilkinson CJ, Nigg EA (2005) The Polo kinase Plk4 functions in centriole duplication. *Nat Cell Biol* **7:** 1140–1146

Hiraki M, Nakazawa Y, Kamiya R, Hirono M (2007) Bld10p constitutes the cartwheel-spoke tip and stabilizes the 9-fold symmetry of the centriole. *Curr Biol* **17:** 1778–1783

Hsu WB, Hung LY, Tang CJ, Su CL, Chang Y, Tang TK (2008) Functional characterization of the microtubule-binding and -destabilizing domains of CPAP and d-SAS-4. *Exp Cell Res* **314:** 2591–2602

Hung LY, Chen HL, Chang CW, Li BR, Tang TK (2004) Identification of a novel microtubule-destabilizing motif in CPAP that binds to tubulin heterodimers and inhibits microtubule assembly. *Mol Biol Cell* **15:** 2697–2706

Hung LY, Tang CJ, Tang TK (2000) Protein 4.1 R-135 interacts with a novel centrosomal protein (CPAP) which is associated with the gamma-tubulin complex. *Mol Cell Biol* **20:** 7813–7825

Hussain MS, Baig SM, Neumann S, Nurnberg G, Farooq M, Ahmad I, Alef T, Hennies HC, Technau M, Altmuller J, Frommolt P, Thiele H, Noegel AA, Nurnberg P (2012) A truncating mutation of CEP135 causes primary microcephaly and disturbed centrosomal function. *Am J Hum Genet* **90:** 871–878

Jerka-Dziadosz M, Gogendeau D, Klotz C, Cohen J, Beisson J, Koll F (2010) Basal body duplication in Paramecium: the key role of Bld10 in assembly and stability of the cartwheel. *Cytoskeleton* **67:** 161–171

Kalay E, Yigit G, Aslan Y, Brown KE, Pohl E, Bicknell LS, Kayserili H, Li Y, Tuysuz B, Nurnberg G, Kiess W, Koegl M, Baessmann I, Buruk K, Toraman B, Kayipmaz S, Kul S, Ikbal M, Turner DJ, Taylor MS *et al* (2011) CEP152 is a genome maintenance protein disrupted in Seckel syndrome. *Nat Genet* **43:** 23–26

Kirkham M, Muller-Reichert T, Oegema K, Grill S, Hyman AA (2003) SAS-4 is a C. elegans centriolar protein that controls centrosome size. *Cell* **112:** 575–587

Kitagawa D, Vakonakis I, Olieric N, Hilbert M, Keller D, Olieric V, Bortfeld M, Erat MC, Fluckiger I, Gonczy P, Steinmetz MO (2011) Structural basis of the 9-fold symmetry of centrioles. *Cell* **144:** 364–375

Kleylein-Sohn J, Westendorf J, Le Clech M, Habedanck R, Stierhof YD, Nigg EA (2007) Plk4-induced centriole biogenesis in human cells. *Dev Cell* **13:** 190–202

Kohlmaier G, Loncarek J, Meng X, McEwen BF, Mogensen MM, Spektor A, Dynlacht BD, Khodjakov A, Gonczy P (2009) Overly long centrioles and defective cell division upon excess of the SAS-4-related protein CPAP. *Curr Biol* **19:** 1012–1018

Kumar A, Girimaji SC, Duvvari MR, Blanton SH (2009) Mutations in STIL, encoding a pericentriolar and centrosomal protein, cause primary microcephaly. *Am J Hum Genet* **84:** 286–290

Kuriyama R, Borisy GG (1981) Centriole cycle in Chinese hamster ovary cells as determined by whole-mount electron microscopy. *J Cell Biol* **91:** 814–821

Leidel S, Delattre M, Cerutti L, Baumer K, Gonczy P (2005) SAS-6 defines a protein family required for centrosome duplication in C. elegans and in human cells. *Nat Cell Biol* **7:** 115–125

Leidel S, Gonczy P (2003) SAS-4 is essential for centrosome duplication in C elegans and is recruited to daughter centrioles once per cell cycle. *Dev Cell* **4:** 431–439

Matsuura K, Lefebvre PA, Kamiya R, Hirono M (2004) Bld10p, a novel protein essential for basal body assembly in Chlamydomonas: localization to the cartwheel, the first ninefold symmetrical structure appearing during assembly. *J Cell Biol* **165:** 663–671

Mottier-Pavie V, Megraw TL (2009) Drosophila bld10 is a centriolar protein that regulates centriole, basal body, and motile cilium assembly. *Mol Biol Cell* **20:** 2605–2614

Nakazawa Y, Hiraki M, Kamiya R, Hirono M (2007) SAS-6 is a cartwheel protein that establishes the 9-fold symmetry of the centriole. *Curr Biol* **17:** 2169–2174

Nigg EA, Stearns T (2011) The centrosome cycle: centriole biogenesis, duplication and inherent asymmetries. *Nat Cell Biol* **13:** 1154–1160

O'Connell KF, Caron C, Kopish KR, Hurd DD, Kemphues KJ, Li Y, White JG (2001) The C. elegans zyg-1 gene encodes a regulator of centrosome duplication with distinct maternal and paternal roles in the embryo. *Cell* **105:** 547–558

Ohta T, Essner R, Ryu JH, Palazzo RE, Uetake Y, Kuriyama R (2002) Characterization of Cep135, a novel coiled-coil centrosomal protein involved in microtubule organization in mammalian cells. *J Cell Biol* **156:** 87–99

Peel N, Stevens NR, Basto R, Raff JW (2007) Overexpressing centriole-replication proteins *in vivo* induces centriole overduplication and *de novo* formation. *Curr Biol* **17:** 834–843

Pelletier L, O'Toole E, Schwager A, Hyman AA, Muller-Reichert T (2006) Centriole assembly in Caenorhabditis elegans. *Nature* **444:** 619–623

Rodrigues-Martins A, Bettencourt-Dias M, Riparbelli M, Ferreira C, Ferreira I, Callaini G, Glover DM (2007) DSAS-6 organizes a tube-like centriole precursor, and its absence suggests modularity in centriole assembly. *Curr Biol* **17:** 1465–1472

Roque H, Wainman A, Richens J, Kozyrska K, Franz A, Raff JW (2013) Drosophila Cep135/Bld10 maintains proper centriole structure but is dispensable for cartwheel formation. *J Cell Sci* **125**(Pt 23): 5881–5886

Schmidt TI, Kleylein-Sohn J, Westendorf J, Le Clech M, Lavoie SB, Stierhof YD, Nigg EA (2009) Control of centriole length by CPAP and CP110. *Curr Biol* **19:** 1005–1011

Singla V, Romaguera-Ros M, Garcia-Verdugo JM, Reiter JF (2010) Ofd1, a human disease gene, regulates the length and distal structure of centrioles. *Dev Cell* **18:** 410–424

Sir JH, Barr AR, Nicholas AK, Carvalho OP, Khurshid M, Sossick A, Reichelt S, D'Santos C, Woods CG, Gergely F (2011) A primary microcephaly protein complex forms a ring around parental centrioles. *Nat Genet* **43:** 1147–1153

Tang CJ, Fu RH, Wu KS, Hsu WB, Tang TK (2009) CPAP is a cell-cycle regulated protein that controls centriole length. *Nat Cell Biol* **11:** 825–831

Tang CJ, Lin SY, Hsu WB, Lin YN, Wu CT, Lin YC, Chang CW, Wu KS, Tang TK (2011) The human microcephaly protein STIL interacts with CPAP and is required for procentriole formation. *EMBO J* **30:** 4790–4804

Thornton GK, Woods CG (2009) Primary microcephaly: do all roads lead to Rome? *Trends Genet* **25:** 501–510

van Breugel M, Hirono M, Andreeva A, Yanagisawa HA, Yamaguchi S, Nakazawa Y, Morgner N, Petrovich M, Ebong IO, Robinson CV, Johnson CM, Veprintsev D, Zuber B (2011) Structures of SAS-6 suggest its organization in centrioles. *Science* **331:** 1196–1199

Vulprecht J, David A, Tibelius A, Castiel A, Konotop G, Liu F, Bestvater F, Raab MS, Zentgraf H, Izraeli S, Kramer A (2012) STIL is required for centriole duplication in human cells. *J Cell Sci* **125:** 1353–1362

